7-2015

Analyzing the Catalytic Role of Active Site Residues in the Fe-type Nitrile Hydratase from *Comamonas testosteroni* Ni1

Salette Martinez
Loyola University Chicago

Rui Wu
Loyola University Chicago

Karoline Krzywda
Loyola University Chicago

Veronika Opalka
Loyola University Chicago

Hei Chan
Loyola University Chicago

See next page for additional authors

Analyzing The Catalytic Role of Active Site Residues in The Fe-Type Nitrile Hydratase from *Comamonas testosteroni* Ni1

Salette Martinez
Department of Chemistry, Marquette University, Milwaukee, WI
Department of Chemistry and Biochemistry, Loyola University Chicago, Chicago, IL
Rui Wu
Department of Chemistry and Biochemistry, Loyola University Chicago, Chicago, IL
Karoline Krzywda
Department of Chemistry and Biochemistry, Loyola University Chicago, Chicago, IL
Veronika Opalka
Department of Chemistry and Biochemistry, Loyola University Chicago, Chicago, IL

Journal of Biological Inorganic Chemistry, Vol 20, No. 5 (July 2015): pg. 885-894. DOI.

Hei Chan
Department of Chemistry and Biochemistry,
Loyola University Chicago,
Chicago, IL
Dali Liu
Department of Chemistry and Biochemistry,
Loyola University Chicago,
Chicago, IL
Richard C. Holz
Department of Chemistry, Marquette University,
Milwaukee, WI

Abstract: A strictly conserved active site arginine residue (αR157) and two histidine residues (αH80 and αH81) located near the active site of the Fe-type nitrile hydratase from *Comamonas testosteroni* Ni1 (*Ct*NHase), were mutated. These mutant enzymes were examined for their ability to bind iron and hydrate acrylonitrile. For the αR157A mutant, the residual activity (k_{cat} = 10 ± 2 s^{-1}) accounts for less than 1 % of the wild-type activity (k_{cat} = 1100 ± 30 s^{-1}) while the K_m value is nearly unchanged at 205 ± 10 mM. On the other hand, mutation of the active site pocket αH80 and αH81 residues to alanine resulted in enzymes with k_{cat} values of 220 ± 40 and 77 ± 13 s^{-1}, respectively, and K_m values of 187 ± 11 and 179 ± 18 mM. The double mutant (αH80A/αH81A) was also prepared and provided an enzyme with a k_{cat} value of 132 ± 3 s^{-1} and a K_m value of 213 ± 61 mM. These data indicate that all three residues are catalytically important, but not essential. X-ray crystal structures of the αH80A/αH81A, αH80W/αH81W, and αR157A mutant *Ct*NHase enzymes were solved to 2.0, 2.8, and 2.5 Å resolutions, respectively. In each mutant enzyme, hydrogen-bonding interactions crucial for the catalytic function of the αCys^{104}-SOH ligand are disrupted. Disruption of these hydrogen bonding interactions likely alters the nucleophilicity of the sulfenic acid oxygen and the Lewis acidity of the active site Fe(III) ion.

Keywords: Nitrile hydratase, Iron Hydrolysis X-ray crystallography

Journal of Biological Inorganic Chemistry, Vol 20, No. 5 (July 2015): pg. 885-894. DOI.

An animated Interactive 3D Complement (I3DC) is available in Proteopedia at: http://proteopedia.org/w/Journal:JBIC:32

Electronic supplementary material

The online version of this article (doi:10.1007/s00775-015-1273-3) contains supplementary material, which is available to authorized users.

Introduction

Nitrile hydratases (NHases, EC 4.2.1.84) catalyze the hydration of nitriles to their corresponding amides under ambient conditions and physiological pH.[1–3] Industrial processes used to hydrate nitriles to amides (either acid or base hydration), are often incompatible with the sensitive structures of many industrially and synthetically relevant compounds. Therefore, NHases have attracted substantial interest as biocatalysts in preparative organic chemistry.[4] NHases are already used in several industrial applications such as the synthesis of specialty chemicals and pharmaceuticals including acrylamide and nicotinamide.[5, 6] A key advantage of NHases is their stereoselectivity, which is of particular importance in the pharmaceutical arena. Moreover, given the exquisite reaction specificity, high turnover number, and benign environmental impact, NHases are becoming increasingly recognized as a "Green" catalyst for the degradation of environmentally harmful nitriles. However, details of their reaction mechanism remain poorly understood, hindering further development and exploitation of both biological and biomimetic nitrile hydrating catalysts.

X-ray crystallographic studies on NHases indicate that they are $\alpha_2\beta_2$ heterotetramers that contain either a non-heme Fe(III) ion (Fe-type) or a non-corrin Co(III) ion (Co-type).[1, 6, 7] The metal ion is ligated by three cysteine sulfur atoms, two backbone amide nitrogens, and a water molecule.[8–11] Two of the active site cysteine residues are post-translationally modified to cysteine-sulfinic acid (Cys-SO_2H) and cysteine-sulfenic acid (Cys-SOH) yielding an unusual metal coordination geometry, termed the "claw-setting".[8, 9] Recently, X-ray crystal structures of a Co-type NHase from *Pseudonocardia thermophila* JCM 3095(*Pt*NHase) bound by butane boronic acid and

Journal of Biological Inorganic Chemistry, Vol 20, No. 5 (July 2015): pg. 885-894. DOI.

phenylboronic acid revealed a covalent bond between the oxygen atom of the sulfenic acid ligand and the boron atom of the boronic acid.[12] These data provided the first experimental evidence that the sulfenic acid ligand can function as a nucleophile, which was supported by DFT calculations[13] and QM/MM studies.[14]

The prevailing dogma is that both Co- and Fe-type NHase enzymes require the co-expression of an activator protein to be soluble and fully active.[15–19] Several open reading frames (ORFs) have been identified just downstream from the structural α- and β-subunit genes of NHases, and one of these genes has been proposed to function as an activator protein.[15–19] However, the Fe-type NHase from *Comamonas testosteroni* Ni1 (*Ct*NHase) is unusual among NHases in that it can incorporate iron into its active site and properly oxidize the equatorial cysteine ligands to Cys^{104}-SOH and Cys^{102}-SO_2H in the absence of an activator protein.[20] The X-ray crystal structure of *Ct*NHase is similar to other Fe-type NHases except that the Fe(III) ion in the active site is solvent exposed and resides at the bottom of an open cavity.[20] Analysis of its crystal structure revealed that two α-subunit histidine residues, αHis80 and αHis81, and an arginine residue, αArg157, interact with a phosphate ion retained in the active site from the crystallization solution (Fig. 1). Both histidine residues are located near the active site within the solvent accessible cavity while the arginine residue forms hydrogen bonds with Cys^{104}-SOH (in *Ct*NHase this residue is observed as a Cys^{104}-SO_2H, due to the conditions used for the crystallization), which was recently shown to be capable of functioning as a nucleophile.[20] Neither histidine residue is conserved among Fe- or Co-type NHases, while the arginine residue is strictly conserved among both types of NHases (Fig. 2).

Journal of Biological Inorganic Chemistry, Vol 20, No. 5 (July 2015): pg. 885-894. DOI.

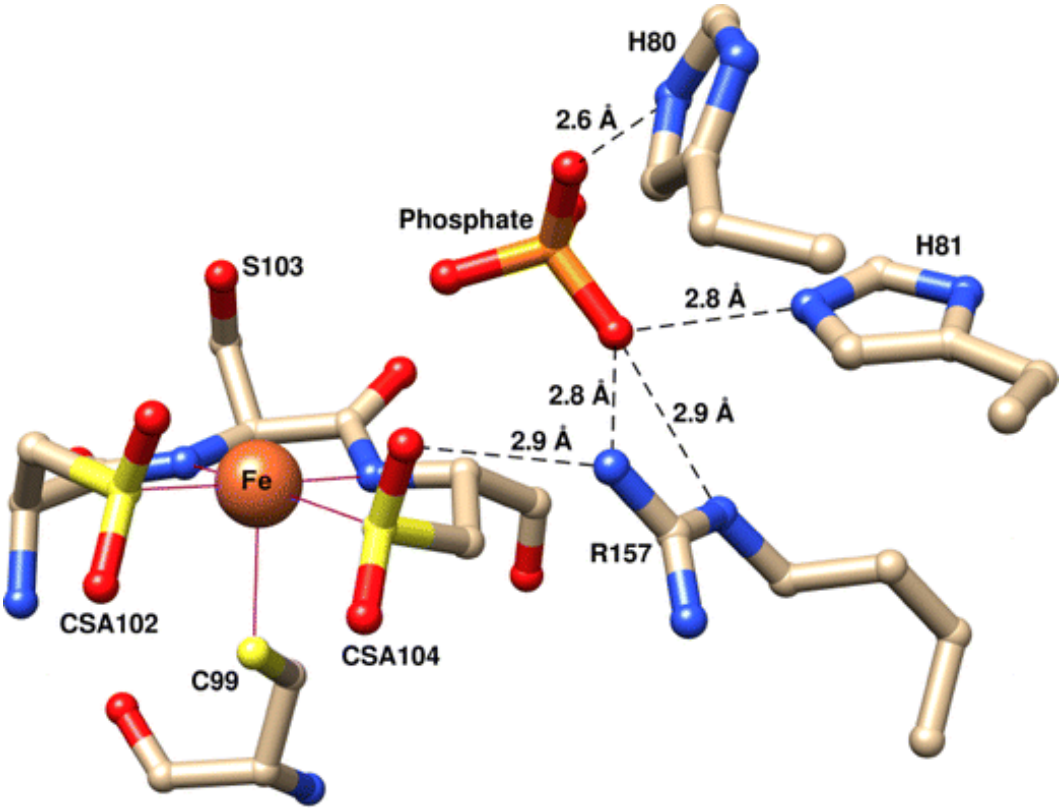

Fig. 1. Active site of wild-type *Ct*NHase (PDB ID: 4FM4) in *ball-and-stick* form. The *black dashed lines* represent the hydrogen bonds

```
Ct          : ---------------MTDNAVMEQRVDALFVLTKELGLVTDQTVPDYEDALMHDWLPQNGAKLVAKAWTDPVFKA :  60
Re-TG328-2  : MSVLIDHAKHTGVPGVPEQAPARDRAWALYEALKSKGAVPDGYVEGWKKTFEEDFTPRKGAELVARAWTDPEFRE :  75
Rh-R312     : MSVTIDHTTENAAPA---QAAVSDRAWALFRALDGKGLVPDGYVEGWKKTFEEDFSPRRGAELVARAWTDPEFRQ :  72
Rh-N771     : -SVTIDHTTENAAPA---QAPVSDRAWALFRALDGKGLVPDGYVEGWKKTFEEDFSPRRGADLVARAWTDPEFRQ :  71
Pt          : MTENILRKSDEEIQK-----EITARVKALESMLIEQGILTTSMIDRMAEIYENEVGPHLGAKVVVKAWTDPEFKK :  70
Rh/HM-J1    : ----MSEHVNKYTEY-------EARTKAIETLLYERGLITPAAVDRVVSYYENEIGPMGGAKVVAKSWVDPEYRK :  64

Ct          : QLLSEGVAASESLGFSFPKHHKHFVVLENTPELHNVICSLCSCTAFTIIGMAPDWYKELEYRARIVRQARTVLK : 135
Re-TG328-2  : LLLTDGTAAVAQYGWLGPQGEY-IVALEDTPTLKNVIVCSLCSCTAWPILGLPPTWYKSFEYRARVVREPRKVLE : 149
Rh-R312     : LLLTDGTAAVAQYGYLGPQGEY-IVAVEDTPTLKNVIVCSLCSCTAWPILGLPPTWYKSFEYRARVVREPRKVLS : 146
Rh-N771     : LLLTDGTAAVAQYGYLGPQGEY-IVAVEDTPTLKNVIVCSLCSCTAWPILGLPPTWYKSFEYRARVVREPRKVLS : 145
Pt          : RLLADGTEACKELGIGGLQGED-MMWVENTDEVHHVVVCTLCSCYPWPVLGLPPNWFKEPQYRSRVVREPRQLLK : 144
Rh/HM-J1    : WLEEDATAAMASLGYAGEQAHQ-ISAVFNDSQTHHVVVCTLCSCYPWPVLGLPPAWYKSMEYRSRVVADPRGVLK : 138

Ct          : -EIGLDLPESIDIRVWDTTADTRYMVLPLRPQGTEDWSEAQLATLITQDCLIGVSRLEAPFAALPAPAVALGA : 207
Re-TG328-2  : -EMGTTLPADTKIRVVDTTAETRYLVIPVRPEGTEGWTAEQLQEIVTKDCLIGVAVPQVP------------ : 208
Rh-R312     : -EMGTEIASDIEIRVYDTTAETRYMVLPQRPAGTEGWSQEQLQEIVTKDCLIGVAIPQVPTV---------- : 207
Rh-N771     : -EMGTEIASDIEIRVYDTTAETRYMVLPQRPAGTEGWSQEQLQEIVTKDCLIGVAIPQVPTV---------- : 206
Pt          : EEFGFEVPPSKEIKVWDSSSEMRFVVLPQRPAGTDGWSEEELATLVTRESMIGVE----PAKAVA-------- : 205
Rh/HM-J1    : RDFGFDIPDEVEVRVWDSSSEIRYIVIPERPAGTDGWSEEELTKLVSRDSMIGVSNALTPQEVIV-------- : 203
```

Fig. 2. Alignment of the amino acid sequences of the α-subunits of Co-type and Fe-type nitrile hydratases. The conserved metal-binding motif and the arginine residue which hydrogen bonds to the active site cysteine-sulfenic acid are highlighted in *black*. The two non-conserved histidine residues (αHis80 and αHis81) found in *Ct*NHase are highlighted in *gray*. Ct, *Comamonas testosteroni* Ni1 (Fe-type); Re-TG3282, *Rhodococcus equi*

Journal of Biological Inorganic Chemistry, Vol 20, No. 5 (July 2015): pg. 885-894. DOI.

TG328-2 (Fe-type); Rh-R312, *Rhodococcus* sp. 312 (Fe-type); Rh-N771, *Rhodococcus* sp. N771 (Fe-type); Pt, *Pseudonocardia thermophila* JCM 3095 (Co-type); Rh/HM-J1, *Rhodococcus rhodochrous* J1 high-molecular-mass (Co-type)

In an effort to understand the roles that αHis80, αHis81, and αR157 play in enzyme maturation and/or catalysis, these residues were mutated to αH80A, αH81A, αH80A/αH81A, αH80W/αH81W, αR157A, and αR157K. Each of these mutant enzymes were investigated via kinetic, inductively coupled mass spectrometry (ICP-MS), UV–Visible spectroscopy. In addition, the X-ray crystal structures of three of the mutant enzymes (αH80A/αH81A, αH80W/αH81W, and αR157A) were solved. Combination of these data provides insight into the role of these residues in metal ion incorporation and catalysis for *Ct*NHase.

Materials and methods

Materials

Acrylonitrile, 2-Amino-2-hydroxymethyl-propane-1,3-diol hydrochloride (Tris–HCl), and 4-(2-hydroxyethyl)piperazine-1-ethanesulfonic acid (HEPES) were obtained from Sigma-Aldrich. All other materials were purchased at the highest quality available.

Expression and purification of CtNHase mutants

Site-directed mutagenesis was performed using the QuikChange Lightning Multi Site-Directed Mutagenesis Kit from Agilent Technologies following the manufacturer's instructions. The expression plasmid pSMCtαβHis containing the α- and β-His_6 genes of *Ct*NHase was used as the template for mutagenesis with the primers listed in Table S1. The mutations were confirmed by DNA sequencing at the University of Chicago Cancer Research Center DNA sequencing facility. Mutant plasmids were transformed into *Escherichia coli* BL21(DE3) competent cells (Agilent Technologies) for expression. Wild-type and mutant *Ct*NHase proteins were expressed and purified by immobilized metal affinity chromatography as previously described for the wild-type protein.[20] Purified protein samples were analyzed by SDS-PAGE.

Journal of Biological Inorganic Chemistry, Vol 20, No. 5 (July 2015): pg. 885-894. DOI.

Protein concentrations were determined using a Coomassie (Bradford) Protein Assay Kit (Thermo Scientific).

Kinetic assay

The activity of wild-type and mutant proteins were determined by following the hydration of acrylonitrile in 50 mM Tris–HCl pH 7.5 spectrophotometrically at 225 nm ($\Delta\varepsilon_{225}$ = 2.9 mM^{-1} cm^{-1}). All assays were performed at 25 °C using a Shimadzu UV-2450 PC spectrophotometer in a 1 mL quartz cuvette with substrate concentrations ranging from 0 to 700 mM. One unit (U) of NHase activity is defined as the formation of 1 μmol of acrylamide per minute. To obtain the kinetic parameters, V_{max} and K_m, the initial velocities from at least two independent measurements were fitted to the Hill equation by non-linear regression using OriginPro 9.0 (OriginLab, Northampton, MA).

Metal analysis and UV–Visible spectroscopy

The metal content of mutant proteins was determined by ICP-MS. Purified wild-type and mutant proteins along with a control of buffer (50 mM Tris–HCl, pH 7.5) containing no protein were treated with concentrated nitric acid and heated at 70 °C for 1 h. The samples were allowed to cool to room temperature then diluted to a final concentration of 5 % nitric acid. The metal content was analyzed at the Water Quality Center in the College of Engineering at Marquette University. UV–Vis absorption spectra were recorded on a Shimadzu UV-2450 PC spectrophotometer in 1 mL quartz cuvettes in 50 mM Tris–HCl, pH 7.5, and 300 mM NaCl at 10 °C.

Crystallization of mutant proteins and data collection

Crystals of *Ct*NHase mutant proteins were obtained by the hanging drop vapor diffusion method using the same conditions as those previously described for the wild-type *Ct*NHase.[20] Optimized conditions were: 1 μl of *Ct*NHase enzyme (15, 20, or 30 mg/ml) in 50 mM HEPES pH 7.0 with an equal volume of the crystallization reservoir solution (1.08 M K_2HPO_4, 0.49 M NaH_2PO_4 with 25 or 30 % (v/v) glycerol). The best quality *Ct*NHase crystals were obtained at

20 °C after ~5 days. For X-ray diffraction data collection, the crystals were flash frozen in liquid nitrogen. Data sets were collected at the SBC 19-ID beamline at the Advanced Photon Source, Argonne National Laboratory (Argonne, IL, USA). Monochromatic data collection was conducted at a wavelength of 0.98 Å using a Quantum 315 CCD detector providing data sets with resolutions ranging from 2.0 to 2.8 Å.

Structure determination and refinement

X-ray data sets for the αH80A/αH81A, αH80W/αH81W, and αR157A *CtNHase* mutant enzymes were indexed, integrated and scaled using HKL3000 software and the statistics revealed that the data were of good quality (Table 1).[21] The space group for each was $P3_1$ with eight copies of *Ct*NHase heterodimers in each asymmetric unit resulting a total solvent content of ~70 %. Molecular replacement was carried out with wild-type *Ct*NHase as the search model (PDB ID: 4FM4)[20] using the program Phaser[22] from the CCP4 software suite.[23] Once a solution was obtained, model building was conducted in COOT;[24] rigid-body refinement and restrained refinement was conducted in refmac5.[25] To remove model bias and achieve the best refinement result possible, simulated annealing refinement, TLS refinement, and ordered solvent identification were conducted using PHENIX.refine[26] while model building continued until the lowest R_{free}/R values were achieved. Active site metal ion occupancies were initially set at one resulting in negative difference electron density ($F_o–F_c$ map) around the metal center (not shown). Metal analyses indicated less than one equivalent of iron per heterodimer, therefore, the final structural model was refined with iron ion occupancies and those of the three coordinating residues (CSA102, S103 and CSA104) set at 0.8. Positive difference electron density ($F_o–F_c$ map) around this region was observed (not shown) after refinement, which is likely due to the contribution of residues 102–104 from the 20 % apo-enzyme molecules in the crystal. The structure was refined using PHENIX.refine with the completed model possessing R_{free}/R values provided in Table 2. Since the $P3_1$ space group could be indicative of twining, the *L*-test for twining was conducted using the Xtriage program in PHENIX revealing that the intensity statistics behave as expected, indicating no twining. Coordinates and structure factors have been deposited in the

Journal of Biological Inorganic Chemistry, Vol 20, No. 5 (July 2015): pg. 885-894. DOI.

Research Collaboratory for Structural Bioinformatics (RCSB) Protein Data Bank (PDB) as entries 4ZGJ (*Ct*NHase αH80A/αH81A), 4ZGE (*Ct*NHase αH80W/αH81W) and 4ZGD (*Ct*NHase αR157A).

Table 1. Data collection and refinement statistics for the *Ct*NHase mutant crystal structures

Data set	***Ct*NHase αH80A/αH81A (PDBID: 4ZGJ)**	***Ct*NHase αH80W/αH81W (PDBID: 4ZGE)**	***Ct*NHase αR157A (PDBID: 4ZGD)**
Space Group	$P3_1$	$P3_1$	$P3_1$
Unit cell dimensions			
$a = b$ (Å)	112.0	111.7	111.6
c (Å)	476.0	475.9	474.6
$\alpha = \beta$ (°)	90	90	90
γ (°)	120	120	120
Resolution (Å)	36.57–2.00	67.84–2.80	50.60–2.25
[a]R_{merge} (%)	14.8 (69.9)	14.5 (72.4)	15.6 (72.4)
R_{pim} (%)	19.0 (32.6)	8.9 (43.4)	9.3 (43.2)
CC_{I_mean}	0.859 (0.473)	0.989 (0.708)	0.988 (0.593)
I/sigma (I)	3.2 (2.2)	7.3 (1.9)	6.9 (2.1)
Completeness (%)	99.7 (99.2)	99.9 (100)	100 (100)
Redundancy	5.6 (5.5)	3.6 (3.7)	3.8 (3.7)
No. total reflections	2,508,285	585,059	1,185,275
No. unique reflections	450,084	163,400	313,740
[b]R_{work}/[c]R_{free} (%)	25.3/21.9	22.9/18.1	20.3/17.3
No. of atoms	30,101	26,101	28,551
No. of solvent atoms	4561	445	2995
Average B-factors (Å^2)			
Overall	30.3	48.4	31.8
Protein main chain	28.5	48.4	30.4
Protein side chain	30.8	48.8	32.4
Solvent	41.7	39.1	37.7
Metal ion	23.6	50.4	32.6
RMSD bond length (Å)	0.002	0.008	0.007
RMSD bond angles (°)	0.73	1.16	1.07
Ramachandran			
Favored (%)	96.4	94.9	96.7
Allowed (%)	2.6	3.8	2.5
Outlier (%)	1.0	1.3	0.8

The values for the highest resolution bin are in parentheses

RMSD root mean square deviation

[a]Linear $R_{merge}=\Sigma|I_{obs}-I_{avg}|/\Sigma I_{avg}$

Journal of Biological Inorganic Chemistry, Vol 20, No. 5 (July 2015): pg. 885-894. DOI.

[b] $R_{work} = \Sigma |F_{obs} - F_{calc}| / \Sigma F_{obs}$

[c] Five percent of the reflection data were selected at random as a test set and only these data were used to calculate R_{free}

Table 2. Kinetic constants for the wild-type and mutant *Ct*NHases

	k_{cat} (s^{-1})	K_m (mM)
Wild-type	1100 ± 30	250 ± 20
αH80A	220 ± 38	187 ± 18
αH81A	77 ± 13	179 ± 11
αH80A/αH81A	132 ± 3	213 ± 61
αH80W/αH81W	79 ± 4	232 ± 7
αR157A	10 ± 2	204 ± 8
αR157K	32 ± 4	239 ± 1

Acrylonitrile was used as the substrate

Results and discussion

The kinetic constants for wild-type *Ct*NHase and the *Ct*NHase mutant enzymes were obtained by monitoring the hydration of acrylonitrile to acrylamide at 225 nm and 25 °C in 50 mM Tris–HCl pH 7.5. The wild-type enzyme exhibited a k_{cat} value of 1,100 ± 30 s^{-1} and a K_m value of 250 ± 20 mM (Table 2). The k_{cat} value obtained is ~15-fold faster than previously reported[20] and is in line with the vast majority of Fe-type NHase enzymes while the K_m value is ~1.4-fold lower.[20] The difference in the observed k_{cat} value is likely due to the rapid purification process employed, which allowed the assay to be performed immediately after the enzyme was purified (both purification and kinetic measurements were performed in a time-window of <12 h), since it was found that *Ct*NHase loses catalytic activity over time.[20] Such a decrease in catalytic activity has been reported for both Co- and Fe-type NHases and likely results from the oxidation of the Cys-SOH ligand to Cys-SO_2H when stored under aerobic conditions and in the absence of butyric acid.[27, 28]

Mutation of the strictly conserved arginine residue (αR157), which forms hydrogen bonds with the active site αCys^{104}-SOH ligand (this residue is observed as αCys^{104}-SO_2H in the crystal structure due to the amount of time the crystals were exposed to air during crystallization), (Fig. 2), to an alanine (αR157A) resulted in a *Ct*NHase enzyme that exhibited a k_{cat} value of 10 ± 2 s^{-1} and a K_m value of

205 ± 10 mM (Table 2). The residual activity accounts for less than 1 % of the wild-type activity while the K_m value is nearly unchanged. Similar results were obtained for the Fe-type NHase from *Rhodococcus* sp N-771 (*Rh*NHase) and the closely related Co-type thiocyanate hydrolase from *Thiobacillus thioparus* THI115 (*Tt*SCNase) upon mutation of this arginine residue.[29–31] Therefore, αR157 is important for the hydration of nitriles, however, it is not strictly required for catalysis. In fact, it was recently reported that deletion of the entire β-protein for the toyocamycin nitrile hydratase from *Streptomyces rimosus* provides an enzyme with ~0.3 % of the observed WT enzyme activity.[32] Based on the crystal structure of wild-type *Ct*NHase, a hydrogen-bond exists between the N2 atom of αR157 and the O1 atom of the αCys^{104}-SO_2H ligand, αCys^{104}-SOH in the active form, (2.9 Å). This αCys^{104}-SOH residue has been proposed to function as the nucleophile in catalysis,[12] and has been suggested to exist in its protonated form at pH 7.5.[33] Mutation of αR157 to lysine (αR157K), a residue that in principle could provide a hydrogen bond to the active site sulfenic acid ligand, resulted in an enzyme with a k_{cat} value of 32 ± 4 s^{-1} and a K_m value of 240 ± 10. These data suggest that the protonation state and stability of the active site sulfenic acid ligand is maintained through hydrogen-bond formation with αR157 and disruption of this hydrogen-bond likely result in deprotonation of the active site sulfenic acid ligand decreasing the ability of the catalytic active site to function.

Mutation of the active site pocket residues, αH80 and αH81 to alanine, resulted in enzymes with k_{cat} values of 220 ± 40 mM and 77 ± 13 s^{-1}, respectively, and K_m values of 187 ± 11 and 179 ± 18 mM (Table 2). The double mutant (αH80A/αH81A) was also prepared and provided an enzyme with a k_{cat} value of 132 ± 3 $s^{-1}$and a K_m value of 213 ± 61 mM. Therefore, both αH80 and αH81 are important for the hydration of nitriles, likely participating in hydrogen-bond networks since they are located in the solvent accessible channel; however they are not essential for catalysis. It was hypothesized that the solvent accessibility of the *Ct*NHase active site, both the large opening and the axial approach direction, provides the necessary access for metal ion incorporation without the use of an activator protein.[20] In an attempt to block the channel leading to the active site, a double mutant containing tryptophan (αH80W/αH81W) was also prepared. This mutant *Ct*NHase enzyme exhibited a k_{cat} value

Journal of Biological Inorganic Chemistry, Vol 20, No. 5 (July 2015): pg. 885-894. DOI.

of 79 ± 4 s^{-1} and a K_m value of 232 ± 7. These data indicate that access to the active site Fe(III) ion is not strongly perturbed but the lack of the histidine residues decreases the enzymes ability to hydrate acrylonitrile.

As catalytic activity is dependent on the active site metal ion, the metal content of wild-type *Ct*NHase and each mutant enzyme was determined by ICP-MS. Iron content of wild-type *Ct*NHase was found to be 1.4 ± 0.2 equivalents of iron per $(\alpha\beta)_2$ heterotetramer. These data are in line with the previously reported value of 1.6 equivalents of iron per $(\alpha\beta)_2$ heterotetramer.[20] ICP-MS analysis of the single point mutants, αH80A, αH81A, αR157A, and αR157K revealed that 2.5 ± 0.2, 1.6 ± 0.2, 2.1 ± 0.2, and 1.3 ± 0.1 equivalents of iron is present per $(\alpha\beta)_2$ heterotetramer, respectively. The double mutant's αH80A/αH81A and αH80W/αH81W contained 1.5 ± 0.2 and 1.2 ± 0.1 equivalents of iron per $(\alpha\beta)_2$, respectively. These data are also consistent with those reported for other Fe-Type NHases, which typically contain between 1.6 and 2.0 iron ions per $(\alpha\beta)_2$ heterotetramer.[34, 35] These data indicate that mutating the active site αHis80, αHis81, and αR157 residues have little or no effect on the incorporation of iron into the active site.

Since metal analysis indicated the Fe(III) is present in the active sites of each mutant enzyme, the UV–visible spectrum of each enzyme was recorded (Fig. 3). Fe-type NHases contain an S → Fe(III) ligand-to-metal-charge-transfer (LMCT) band at ~700 nm whose position is a good reporter for electronic perturbations occurring at the metal center that are the result of primary and/or secondary coordination sphere changes.[1] All of the *Ct*NHase mutants exhibited an S → Fe(III) LMCT band with a λ_{max} near 700 nm; however, for αH80A, αH81A, αR157A, and αR157K this absorption band was red-shifted with a corresponding increase in molar absorptivity (ε) (Table S2). On the other hand, the αH80A/αH81A and αH80W/αH81W mutant enzymes exhibited a blue-shift along with an increase in molar absorptivity (Table S2). The observed red-shifts in this LMCT band are typically observed when (i) the pH is increased, (ii), upon interaction with an inhibitor such as butyric acid, (iii), changes in hydrogen-bonding at or near the active site or (iv) oxidation of αCys-SOH to αCys-SO_2H[1, 36, 37] On the other hand, blue-shifts are observed by the addition of substrate and also upon disruption of the hydrogen-bonding network between βArg56 and

Journal of Biological Inorganic Chemistry, Vol 20, No. 5 (July 2015): pg. 885-894. DOI.

Cys^{114}-SOH and βArg56 and Cys^{112}-SO_2H in the Fe-Type NHase from *Rhodococcus* sp. N-771.[38–40] These observed shifts have been attributed to a change in the π-back-donation from the axial cysteine ligand to the metal center, in response to perturbations at the active site.[41, 42]

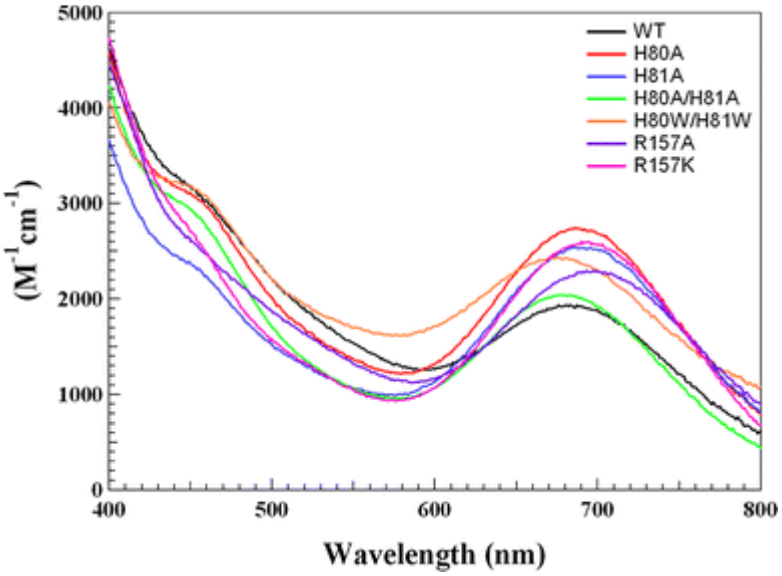

Fig. 3. UV-Visible absorption spectra of wild-type and mutant *Ct*NHases. Spectra were recorded in 50 mM Tris–HCl, pH 7.5, and 300 mM NaCl

Mutation of αR157 to an alanine would result in loss of the hydrogen-bond between the nitrogen atom of the guanidinium moiety of αR157 and the O1 oxygen atom of αCys^{104}-SO_2H (2.9 Å) (Fig. 1). The lack of this hydrogen bond likely results in a decrease in negative charge on the sulfenic acid oxygen as this oxygen has been suggested to be protonated at pH 7.5.[33] This would result in an increase in electron donation to the Fe(III) center from the sulfenic acid sulfur ligand. As a consequence of this change in π-electron donation from the sulfenic acid sulfur ligand, the amount of π-electron donation from the axial thiolate ligand to the Fe(III) ion would likely decrease. A decrease in π-electron donation from the axial thiolate ligand has been attributed to observed red shifts of similar magnitude in the S → Fe(III) LMCT band of several Fe-type NHase enzymes.[41, 42] In contrast, the αR157K enzyme could still participate in hydrogen-bonding with active site sulfenic acid ligand, albeit less efficiently, thus the observed red shift is smaller in magnitude (Table S2). While no direct hydrogen bond is observed between αH80 or αH81 and the active site ligands, they do form hydrogen bonds with solvent

Journal of Biological Inorganic Chemistry, Vol 20, No. 5 (July 2015): pg. 885-894. DOI.

molecules that in turn interact with active site ligands. Therefore, the observed shifts are likely the result of disruption of hydrogen-bonds, hydrogen-bond networks, or the oxidation of αCys^{104}-SOH to αCys^{104}-SO_2H. Oxidation of the sulfenic acid is unlikely given that these spectra were all recorded immediately after purification and the enzyme remained fully active.

To gain insight into the structural perturbations that occur in and around the *Ct*NHase active site upon the mutation of αH80, αH81, and αR157, three mutant enzymes were crystallyzed, αH80A/αH81A, αH80W/αH81W, and αR157A. The X-ray crystal structures of these three *Ct*NHase enzymes were solved to 2.0, 2.8, and 2.25 Å resolutions, respectively. Overall, the X-ray crystal structures of all three mutant *Ct*NHase enzymes are similar to the wild-type structure (Fig. 4a) with the α-carbon root mean squared deviation (rmsd) for the α-subunit within 0.57 Å (αH80A/αH81A), 0.55 Å (αH80W/αH81W), and 0.22 Å (αR157A) and the rsmd for the β-subunit is within 0.23 Å (αH80A/αH81A), 0.19 Å (αH80W/αH81W), and 0.17 Å (αR157A). Three pronounced differences are observed among the α-subunits of all three mutant enzymes. The first is the orientation of the C-terminus (Fig. 4a), which may simply not bear functional significance. The second is a loop regions that contains residues α74–82, while the third is a loop region containing residues α152–155 (Fig. 4b, Table S3). These two loops regions are located in the vicinity of the metal center and near the mutation sites. A loop region in the β-subunit containing residues β92–98 is also slightly perturbed (Fig. 4a). The observed shift in the α74–82 loop region (Fig. 4b, Table S3) in the mutant enzymes, contribute to a much wider channel leading to the active site allowing even greater solvent and substrate access. In addition, a significant change in the orientation of two lysine residues located on this loop, αK79 and αK82, is also observed in the αH80A/αH81A and αH80 W/αH81 W structures (Figure S1). In both structures, the side chains of the two lysine residues change conformation as they flip and point away from the channel compared to the wild-type structure (Figure S1). Such a change in conformation, likely results in the loss of hydrogen-bonding interactions within the active site cavity. Similar perturbations in the hydrogen-bonding networks around the active sites of both Fe- and Co-type NHases have been reported when, for example, second- or third-shell residues in either the α- or β-subunit have been mutated, yielding enzymes with low catalytic activities.[36, 43]

Journal of Biological Inorganic Chemistry, Vol 20, No. 5 (July 2015): pg. 885-894. DOI.

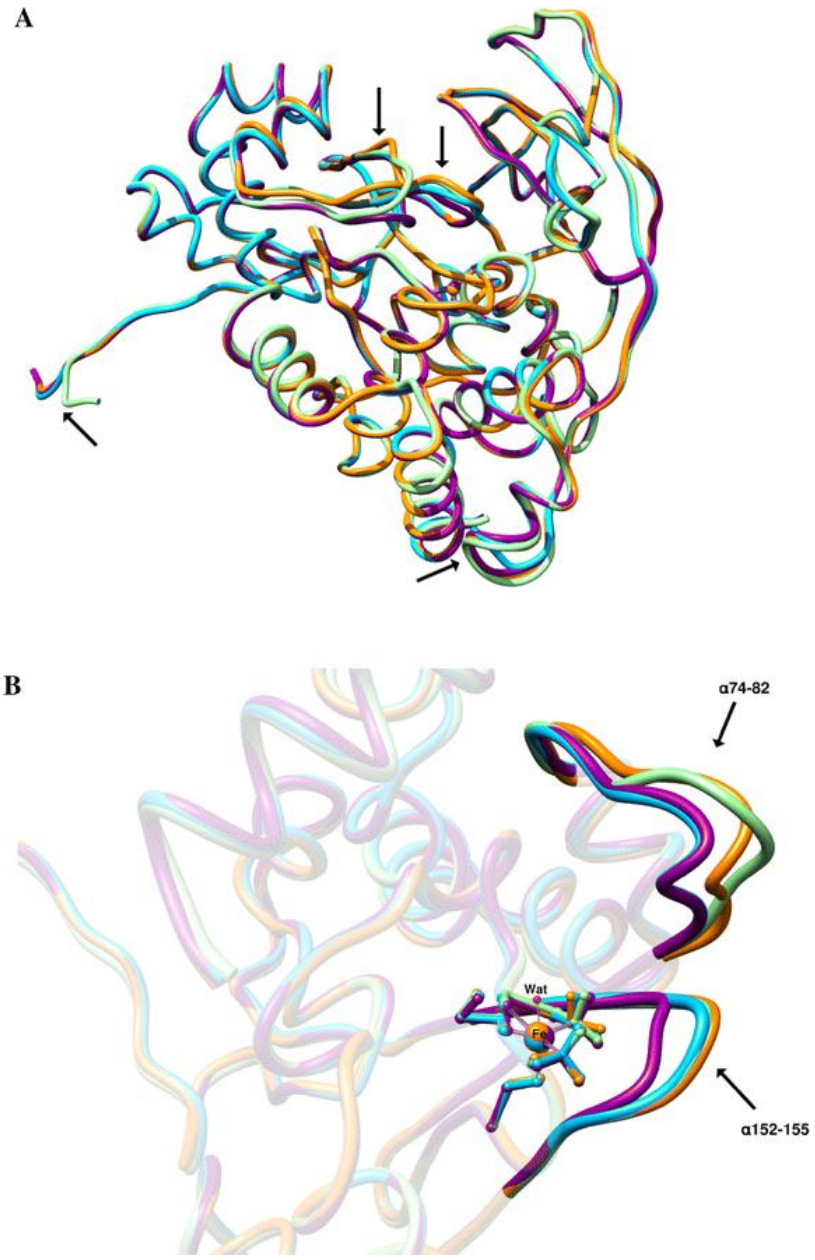

Fig. 4. Superposition of wild-type *Ct*NHase (PDB ID: 4FM4) and mutant structures. **a** Superposition of the αβ heterodimer, the wild-type is in *dark magenta*, αH80A/αH81A mutant is in *light green*, αH80W/αH81W is in *orange*, and the αR157A mutant is in *light blue*. The regions with pronounced difference between the wild-type and the mutant enzymes are indicated with *black arrows*. **b** The two loop regions located in the α-subunit exhibiting relatively significant structural differences are indicated by *black arrows*

The active site Fe(III) ions of the three *Ct*NHase mutants, αH80A/αH81A, αH80W/αH81W, and αR157A are similar to that of the wild-type enzyme in that they are bound by three sulfurs from αC99,

Journal of Biological Inorganic Chemistry, Vol 20, No. 5 (July 2015): pg. 885-894. DOI.

αC102, and αC104, and two backbone amide nitrogens (Fig. 5). No electron density was observed for an exogenous ligand coordinated to the metal ion trans to αC99 ligand in either the αH80W/αH81W or αR157A structures. However, electron density was observed trans to the αC99 ligand and interpreted as a water molecule in the αH80A/αH81A structure (Fig. 5b). Similar to the wild-type enzyme, the equatorial αC102 and αC104 ligands are fully oxidized to αCys-SO_2H in all three mutant structures since the crystals were obtained under aerobic conditions over the course of a week. Interestingly, the phosphate ion, originally present in the active site of the wild-type *Ct*NHase enzyme is absent in all three structures.

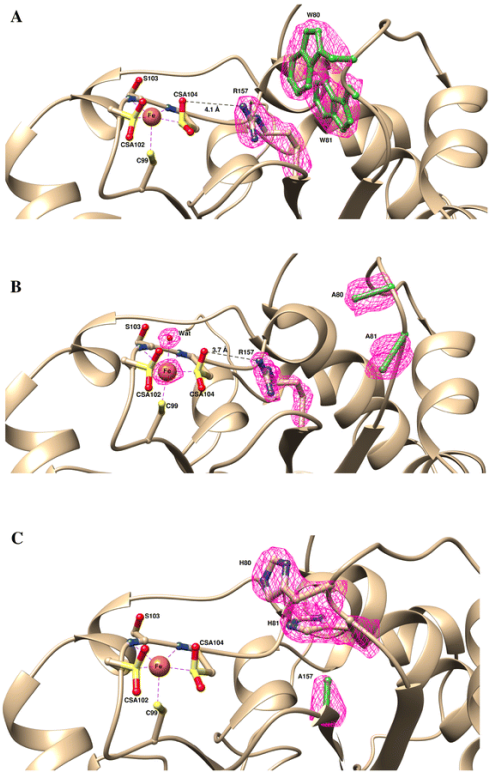

Fig. 5. Active site structures of the mutant enzymes in *ball-and-stick* form with mutated residues shown in *green*. **a** Active site of the αH80W/αH81W mutant with electron density maps ($2F_o - F_c$) shown in *pink* around αR157 and the mutated residues, αH80W and αH81W. **b** Active site of the αH80A/αH81A mutant with with $2F_o - F_c$ electron density map (*pink*) around the αR157, the iron ion, a water molecule, and the mutated residues, αH80A and αH81A. **c** Active site of the αR157A mutant *Ct*NHase with $2F_o - F_c$ electron density map (*pink*) around the mutated residue αR157A, αH80, and αH81. The *black dashed lines* represent hydrogen bonds

The hydrogen-bond observed between the N2-atom of αR157 and the O1-atom of αCys^{104}-SO_2H (αCys^{104}-SOH in the active form) in

Journal of Biological Inorganic Chemistry, Vol 20, No. 5 (July 2015): pg. 885-894. DOI.

the wild-type enzyme is measured at 2.9 Å; however, in the αH80A/αH81A mutant, this distance increases to 3.7 Å (Fig. 5b) while in the αH80W/αH81W enzyme it increases to 4.1 Å (Fig. 5a), both of which are outside a typical hydrogen-bond distance. Although αR157 in both the αH80A/αH81A and αH80W/αH81W mutant enzymes is still capable of forming a hydrogen-bond with the O1 oxygen atom of αCys^{104}-SO_2H (αCys^{104}-SOH in the active form), substitution of αH80 and αH81 for alanine or tryptophan residues disrupts loops α74–82 (Fig. 4a, Table S3) and α152–155 (Fig. 4b, Table S3) resulting in αR157 being pulled away from αCys^{104}-SO_2H (αCys^{104}-SOH in the active form), preventing hydrogen-bond formation. Based on sulfur K-edge EXAFS and geometry-optimized DFT calculations, the protonation state of the sulfenic acid was suggested to be Cys-SOH.[33] Therefore, the loss of this hydrogen bond between αR157 and the O1-atom of the sulfenic acid ligand will likely decrease the nucleophilicity of the sulfenic oxygen atom, consistent with the observed blue-shift in the S → Fe(III) LMCT band. Since the sulfenic acid ligand has been shown to be capable of functioning as the nucleophile in the catalytic reaction,[12] the loss of the hydrogen bond between the αR157 and the O1-atom of the sulfenic acid ligand would be expected to significantly decrease the activity. Therefore, the 10-fold decrease in k_{cat} observed for both αH80A/αH81A and αH80W/αH81W mutant enzymes is consistent with these crystallographic data.

Interestingly, besides the loss of the hydrogen bond between the N2-atom of αR157 and the O1-atom of αCys^{104}-SO_2H (Fig. 5C), the αR157A enzyme has the least structural change in the overall α-subunit (rmsd of 0.225) and the α74–82 loop region (rmsd of 0.320). These data suggest that the >100-fold decrease in the catalytic activity is due to the loss of the hydrogen-bond between αR157 and αCys^{104}-SOH ligand, which has been suggested to function as the nucleophile in the catalytic reaction.[12] That hydrogen-bond formation to the active site cysteine ligands is catalytically important, is also reflected in studies done on both Fe- and Co-type NHases. For example, mutation of αR56 in the Fe-Type NHase from *Rhodococcus erythropolis* N771, which forms a hydrogen bond to both the sulfenic acid and sulfinic acid residues, resulted in an enzyme that exhibits only 1 % of the catalytic activity of the wild-type NHase.[29, 43] Similarly, mutation of αR170 in the Co-Type NHase from *Pseudomonas putida*, which corresponds to the mutated αR157 in *Ct*NHase, to an aspartate

resulted in an enzyme with a 1.6-fold decrease in the catalytic efficiency.[29, 43] These data underscore the importance of hydrogen-bond formation between second sphere residues and the active site sulfinic and sulfenic acid ligands in NHases.

Summary

Mutation of αH80, αH81, and αR157 result in *Ct*NHase enzymes with diminished catalytic activity, indicating that all three residues are catalytically important but not essential. In each mutant enzyme, hydrogen-bonding interactions crucial for the catalytic function of the αCys^{104}-SOH ligand are disrupted. Eliminating these hydrogen bonding interactions likely alters the nucleophilicity of the sulfenic acid oxygen and the Lewis acidity of the active site Fe(III) ion. Several studies on both Fe- and Co-Type NHases have shown the importance of the stability and integrity of the Cys-SOH ligand for catalytic activity in NHases; for example, further oxidation to Cys-SO_2H leads to inactivation.[27, 37] Most recently, in our studies with the Co-Type NHase from *P. thermophila* JCM 3095, we showed that Cys-SOH can function as a nucleophile in the hydration of nitrile to amides by NHase.[12] Therefore stabilization of αCys^{104}-SOH in *Ct*NHase through hydrogen-bond formation with αR157 is important for a fully functional NHase enzyme. Second, although not directly involved in catalysis, the two non-conserved αH80 and αH81 residues appear to play an important role in maintaining the proper structure of the α-subunit in and around the active site. For example, the αH80A/αH81A and αH80W/αH81W mutant enzymes exhibited two significant structural changes in two loop regions of the α-subunit (α74–82 and α152–155) that affected the hydrogen-bonding interaction between αR157 and αCys^{104}-SOH. Therefore, these studies indicate that a combination of elements that include, the proper structure of the active site (i.e. stabilization of active site nucleophile through hydrogen-bonding), proper architecture of the α-subunit, and outer-sphere residues (e.g. αHis80 and αHis81), are necessary for NHase to efficiently catalyze nitrile to amides.

Acknowledgments

This work was supported by the National Science Foundation (CHE-1412443, RCH and CHE-1308672, DL). HC gratefully

acknowledges the ACS Project SEED for funding a summer internship. GM/CA @ APS has been funded in whole or in part with federal funds from the National Cancer Institute (ACB-12002) and the National Institute of General Medical Sciences (AGM-12006).

Supplementary material

775_2015_1273_MOESM1_ESM.docx (497 kb)
ESM1 (DOCX 497 kb)

References

1. Kovacs JA (2004) Chem Rev 104:825–848
2. Yamada H, Kobayashi M (1996) Biosci Biotechnol Biochem 60:1391–1400
3. Brady D, Beeton A, Zeevaart J, Kgaje C, Rantwijk F, Sheldon RA (2004) Appl Microbiol Biotechnol 64:76–85
4. Wang M-X (2005) Top Catal 35:117–130
5. Velankar H, Clarke KG, Preez RD, Cowan DA, Burton SG (2010) Trends Biotechnol 28:561–569
6. Prasad S, Bhalla TC (2010) Biotechnol Adv 28:725–741
7. Harrop TC, Mascharak PK (2004) Acc Chem Res 37:253–260
8. Nagashima S, Nakasako M, Dohmae N, Tsujimura M, Takio K, Odaka M, Yohda M, Kamiya N, Endo I (1998) Nat Struct Mol Biol 5:347–351
9. Miyanaga A, Fushinobu S, Ito K, Wakagi T (2001) Biochem Biophys Res Commun 288:1169–1174
10. Hourai S, Miki M, Takashima Y, Mitsuda S, Yanagi K (2003) Biochem Biophys Res Commun 312:340–345
11. Huang W, Jia J, Cummings J, Nelson M, Schneider G, Lindqvist Y (1997) Structure 15:691–699
12. Martinez S, Wu R, Sanishvili R, Liu D, Holz R (2014) J Am Chem Soc 136:1186–1189
13. Hopmann KH (2014) Inorg Chem 53:2760–2762
14. Kayanuma M, Hanaoka K, Shoji M, Shigeta Y (2015) Chem Phys Lett 623:8–13
15. Nishiyama M, Horinouchi S, Kobayashi M, Nagasawa T, Yamada H, Beppu T (1991) J Bacteriol 173:2465–2472
16. Hashimoto Y, Nishiyamaa M, Horinouchia S, Beppuab T (1994) Biosci Biotechnol Biochem 58:1859–1869
17. Nojiri M, Yohda M, Odaka M, Matsushita Y, Tsujimura M, Yoshida T, Dohmae N, Takio K, Endo I (1999) J Biochem 125:696–704
18. Petrillo KL, Wu S, Hann EC, Cooling FB, Ben-Bassat A, Gavagan JE, DiCosimo R, Payne MS (2005) Appl Microbiol Biotechnol 67:664–670

19. Wu S, Fallon RD, Payne MS (1997) Appl Microbiol Biotechnol 48:704–708
20. Kuhn ML, Martinez S, Gumataotao N, Bornscheuer U, Liu D, Holz RC (2012) Biochem Biophys Res Commun 424:365–370
21. Z. Otwinowski and W. Minor (1997) In: Charles W. Carter, Jr. (ed) Methods enzymol. Academic Press, pp. 307–326
22. McCoy AJ, Grosse-Kunstleve RW, Adams PD, Winn MD, Storoni LC, Read RJ (2007) J Appl Crystallogr 40:658–674
23. N. Collaborative Computational Project (1994) Acta Crystallogr Sect D Biol Crystallogr 50:760–763
24. Emsley P, Cowtan K (2004) Acta Crystallogr Sect D: Biol Crystallogr 60:2126–2132
25. Murshudov GN, Vagin AA, Dodson EJ (1997) Acta Crystallogr Sect D: Biol Crystallogr 53:240–255
26. Adams PD, Grosse-Kunstleve RW, Hung L-W, Ioerger TR, McCoy AJ, Moriarty NW, Read RJ, Sacchettini JC, Sauter NK, Terwilliger TC (2002) Acta Crystallogr Sect D: Biol Crystallogr 58:1948–1954
27. Murakami T, Nojiri M, Nakayama H, Dohmae N, Takio K, Odaka M, Endo I, Nagamune T, Yohda M (2000) Protein Sci 9:1024–1030
28. Arakawa T, Kawano Y, Katayama Y, Nakayama H, Dohmae N, Yohda M, Odaka M (2009) J Am Chem Soc 131:14838–14843
29. Piersma SR, Nojiri M, Tsujimura M, Noguchi T, Odaka M, Yohda M, Inoue Y, Endo I (2000) J Inorg Biochem 80:283–288
30. Endo I, Nojiri M, Tsujimura M, Nakasako M, Nagashima S, Yohda M, Odaka M (2001) J Inorg Biochem 83:247–253
31. Yamanaka Y, Arakawa T, Watanabe T, Namima S, Sato M, Hori S, Ohtaki A, Noguchi K, Katayama Y, Yohda M, Odaka M (2013) J Biosci Bioeng 116:22–27
32. Nelp MT, Astashkin AV, Breci LA, McCarty RM, Bandarian V (2014) Biochemistry 53:3990–3994
33. Dey A, Chow M, Taniguchi K, Lugo-Mas P, Davin S, Maeda M, Kovacs JA, Odaka M, Hodgson KO, Hedman B, Solomon EI (2006) J Am Chem Soc 128:533–541
34. Odaka M, Noguchi T, Nagashima S, Yohda M, Yabuki S, Hoshino M, Inoue Y, Endo I (1996) Biochem Biophys Res Commun 221:146–150
35. Tsujimura M, Dohmae N, Odaka M, Chijimatsu M, Takio K, Yohda M, Hoshino M, Nagashima S, Endo I (1997) J Biol Chem 272:29454–29459
36. Yamanaka Y, Hashimoto K, Ohtaki A, Noguchi K, Yohda M, Odaka M (2010) J Biol Inorg Chem 15:655–665
37. Tsujimura M, Odaka M, Nakayama H, Dohmae N, Koshino H, Asami T, Hoshino M, Takio K, Yoshida S, Maeda M, Endo I (2003) J Am Chem Soc 125:11532–11538

Journal of Biological Inorganic Chemistry, Vol 20, No. 5 (July 2015): pg. 885-894. DOI.

38. Sugiura Y, Kuwahara J, Nagasawa T, Yamada H (1987) J Am Chem Soc 109:5848–5850
39. Miyanaga A, Fushinobu S, Ito K, Shoun H, Wakagi T (2004) Eur J Biochem 271:429–438
40. Gumataotao N, Kuhn ML, Hajnas N, Holz RC (2013) J Biol Chem 288:15532–15536
41. Lugo-Mas P, Dey A, Xu L, Davin SD, Benedict J, Kaminsky W, Hodgson KO, Hedman B, Solomon EI, Kovacs JA (2006) J Am Chem Soc 128:11211–11221
42. Kennepohl P, Neese F, Schweitzer D, Jackson HL, Kovacs JA, Solomon EI (2005) Inorg Chem 44:1826–1836
43. Brodkin HR, Novak WRP, Milne AC, D'Aquino JA, Karabacak NM, Goldberg IG, Agar JN, Payne MS, Petsko GA, Ondrechen MJ, Ringe D (2011) Biochemistry 50:4923–4935